NASA

Technical Memorandum 80627

The Occurrence Rate, Polarization Character, and Intensity of Broadband Jovian Kilometric Radiation

M. D. Desch and M. L. Kaiser

JANUARY 1980

National Aeronautics and Space Administration

Goddard Space Flight Center
Greenbelt, Maryland 20771

THE OCCURRENCE RATE, POLARIZATION CHARACTER AND INTENSITY OF BROADBAND JOVIAN KILOMETRIC RADIATION

M. D. Desch
M. L. Kaiser
NASA/Goddard Space Flight Center
Laboratory for Extraterrestrial Physics
Planetary Magnetospheres Branch
Greenbelt, Maryland 20771

Abstract

We describe the major observational features of one new component of Jupiter's radio emission spectrum, the broadband kilometer-wavelength radiation or bKOM. This study, using the Voyager Planetary Radio Astronomy experiments, reveals that the overall occurrence morphology, total power, and polarization character of bKOM are strong functions of the latitude and/or local time geometry of the observations. The post-encounter data show a decline in the mean occurrence rates and power level of bKOM and, in particular, a depletion in the occurrence rate at those same longitudes where the detection rate is a maximum before encounter. Additionally, the polarization sense undergoes a permanent reversal in sign after encounter, whereas the time-averaged wave axial ratio and degree of polarization remain relatively unchanged. Finally, no evidence of any control by Io is found. The strong dependence of the morphology on local time suggests a source whose beam is nearly fixed relative to the Jupiter-sun line.

Introduction

One of the unexpected results from the Voyager program was the detection of a new component of Jovian radio emission at, typically, kilometric wavelengths [Warwick et al., 1979a; Scarf et al., 1979]. These emissions actually appear in two different forms on frequency-time spectrograms (Warwick et al., 1979b). One form, which is always narrow banded and is quite probably a separate and distinct phenomenon altogether, is described for the first time as such by Kaiser and Desch (1980). The other form is relatively broadband emission, often with a tapered appearance on dynamic spectra. It is this emission, referred to as bKOM, which is discussed here. This bKOM component also has been reported on by Warwick et al. (1979a), Kurth et al. (1979, 1980) and Green and Gurnett (1980).

bKOM consists of strongly polarized stormlike bursts, sometimes exceeding 10^9 watts, and lasting up to 3-4 hrs. These bursts extend from well below 100 kHz to occasionally more than 1000 kHz, with intensity and

duration generally decreasing with increasing frequency above 100 kHz. In data recorded before Jupiter encounter, bKOM has a high occurrence probability of detection when the system III longitude containing Jupiter's north dipole tip ($\sim 200^{\circ}$) faces the spacecraft, and a secondary occurrence maximum at 20° to 40° system III. Some limited evidence [Kurth et al., 1979] indicates the possible direct influence of Io on the occurrence statistics. The bKOM source location has been speculated to be either the Io plasma torus or the Jovian auroral ionosphere [Warwick et al., 1979b; Green and Gurnett, 1980].

The above picture is based largely on observations made prior to spacecraft encounters with Jupiter. Examination of post-encounter data and closer examination of pre-encounter data, however, has revealed significant morphological changes which we attribute to the different observing perspectives of the two spacecraft. Over the period of time under study, the pre-encounter observations were made at approximately 10-1/2 hr local time and 3° Jovigraphic latitude for Voyager 1 (V1) and at about 9-1/2 hr local time and 7° latitude for Voyager 2 (V2) (12 hr local time corresponds to the dayside of Jupiter-sun line; 9 hr is 45° east of this line, toward the dawn terminator). The V1 post-encounter perspective is quite different, corresponding to a local time near 4 hr and a Jovigraphic latitude of $5\text{-}1/2^{\circ}$. We will show that the bKOM dynamic spectra, occurrence statistics, polarization sense, and total power vary in important ways depending on observing perspective. We will also show that there is essentially no correlation between the occurrence of bKOM and the position of Io.

Observations: Occurrence Statistics

The two identical PRA instruments have been fully described by Warwick et al. [1978]. For our purpose here, it is sufficient to say that they include swept-frequency receivers covering the band from 1.2 to 1326.0 kHz in 70 equally spaced steps and a pair of orthogonally mounted 10-m monopoles connected to provide measurement of the right-hand (RH) and left-hand (LH) circularly polarized wave components.

The PRA instruments first detected bKOM in late April and early May 1978 at more than 2 AU from Jupiter. By the time each Voyager had reached ~ 1 AU from Jupiter (October 1978 for Voyager-1 and December 1978 for Voyager-2), detection of bKOM became routine, to the extent that the unmistakable tapered signatures of bKOM events appeared rotation after rotation.

For example, Figure 1 shows V2 dynamic spectra over eight successive Jovian rotations. It is important to note that these observations were made prior to encounter with Jupiter. The lower panel displays total power encoded so that increasing darkness is proportional to increasing power. The top panel shows the sense of polarization with LH represented by black, RH by white, and unpolarized by gray. The tapered events centered near the tic marks indicating the longitude containing the north dipole tip (~ 200°) are bKOM events. It is clear that bKOM is distinct from the higher frequency emissions (hectometric wavelengths - HOM), as if the two bands of emission were anticorrelated.

Although it is clear from Figure 1 that the preferred CML for detection of bKOM is 200°, this is only an approximation. In fact, there are important variations in the System III longitude (CML) occurrence statistics of bKOM from one observing perspective to another. For example, examination of post-encounter data shows a marked change in the dynamic spectrum of bKOM. In Figure 2, we show three successive events detected by V1 on April 8, only the first of which, at ~ 02 hr SCET, appears tapered in appearance with a peak near 200° CML. The other two, centered at about 12 hr and 22 hr SCET, are more characteristic of post-encounter conditions. For these latter two events, the emission is strongest near 150° CML and ceases almost entirely as 200° longitude is approached. This is followed by secondary, weaker emission near 240° longitude. The V2 post-encounter spectra are virtually identical to these latter two V1 events. No spectra resembling this behavior were observed in pre-encounter data from either spacecraft.

The long-term statistical evidence for changes in the System III occurrence of bKOM with observing geometry is presented in Figure 3.

Here we show the V1 and V2 pre-encounter and the V1 post-encounter periods separately. Plotted are "time line" versions of the bKOM activity at 97 kHz in the CML-Io phase space in each lower panel, and absolute occurrence probability histograms at the same frequency in the upper panels. We display results at a single frequency because for the purposes of this paper the histograms at other frequencies differ in only minor details. The time-line plots display all the recorded bKOM activity, and are intended principally to show the occurrence behavior in Io phase. The longitude histograms, however, show events which exceeded two flux density levels, 2.5×10^{-21} (shaded) and 2.5×10^{-22} W m^{-2} Hz^{-1} (unshaded) and are thus intercomparable in an unbiased fashion. The latter value is close to, but comfortably above, the range of detection thresholds which obtain over the duration of each observing period. All measurements of flux density have been normalized to the standard earth-Jupiter opposition distance of 4.04 AU.

Note that for all three observing geometries it is generally true that the detection of bKOM is most likely to occur between about 120° and 280° CML, that is, in the longitude sector centered on or about the longitude containing Jupiter's north magnetic dipole tip. However, the V1 post encounter plot (third panel) shows a pronounced dip near 200° with separate and distinct peaks at 150° and 240° CML. This was to be expected, of course, following the discussion of Figure 2. This plot differs markedly from the before-encounter V1 data, which exhibits a single, symmetric main peak at 210° CML. The rather high level of activity outside the preferred longitude sector in this plot is due to the false identification of a large number of narrow-band KOM (nKOM) events (which were filtered out of the post-encounter data), which we now believe to be a separate phenomenon (Kaiser and Desch, 1980). This pre-encounter V1 plot differs, in turn, in a subtle but very important manner from the pre-encounter V2 data shown in the first panel. The V2 longitude peak is quite asymmetric and may be interpreted as arising from two separate peaks, a minor one at 160° CML adjacent to a major peak at 230° CML. But for the relative amplitudes of the two peaks and the depth of the intervening null, the V2 pre-encounter histogram is reminiscent of the V1 post-encounter result.

Besides manifesting distinctly different longitude signatures, the data sets also vary substantially with regard to their absolute occurrence probablities. Reference to the probability scales in Figure 3 shows that the V2 pre-encounter data show by far the highest detection rate at both flux density levels. Events just above threshold, for example, were detected at a rate of nearly 80% by V2 inbound over the 10° wide longitude sector centered at 225° CML. These observations were also made at the highest Jovigraphic latitude--approximately 7° vs. 3° and 5.5° for the V1 pre- and post-encounter observations respectively. The implication here of a strong latitude dependence in the probability of detecing bKOM is also borne out by the average absolute occurrence probabilities, found by summinng the probabilities of the unshaded histograms from 120° to 270° CML and dividing by the number of bins. The V2 pre-encounter period is found to have the highest occurrence rate, equal to 51%. The V1 post-encounter rate, on the other hand, is only 27%, which is exceeded only slightly by the V1 pre-encounter rate of 31%.

As a final note concerning the occurrence statistics, it is clear from the CML-Io phase plots in Figure 3, that we find no evidence for concentrations of activity at any Io phase locations. Although not shown here, we have also explored the possibility of second order effects by Io, such as might appear as an intensity modulation of the emission, similar to what is observed in the decameter wavelength band. Again, no modulation by Io is apparent.

Polarization State

Although we would like to completely specify the polarization state of the bKOM, the PRA instrumentation configuration allows us to measure unambiguously only the wave polarization sense, that is, whether the approaching wave electric vector rotates in the clockwise (LH) or counterclockwise (RH) direction. In spite of this restriction we will report not only on the polarization sense measurements, but also on wave ellipticity (axial ratio) and percentage polarization observations, keeping strict note of the assumptions and limitations inherent in such measurements.

In a previous paper [Warwick et al., 1979a], we stated that the polarization sense of the north-dipole-tip associated bKOM was usually left-handed. At that time we refrained from making an unequivocal statement concerning the polarization sense because only the V1 data had been examined in detail, and the inbound observing geometry of that spacecraft results in a degradation of the measured wave polarization purity. After examining V2 before-encounter data, however, it has become clear that the north-source bKOM is unquestionably LH polarized. Individual events, lasting anywhere from tens of minutes to several hours, are almost entirely LH polarized from beginning to end and over their entire frequency extent. This is clearly evidenced, for example, by the eight successive bKOM events shown in Figure 1, where the polarization sense is illustrated in the top panel by a black and white code. The bKOM events, which are coincident with the tic marks showing north dipole tip passage, are predominantly black, indicating LH polarization.

Following the encounter of V1 with Jupiter, we observed a reversal in the polarization sense of bKOM. That is, at the same time that V2 observed LH polarized bKOM on the sunward side of Jupiter, V1 observed RH polarized bKOM on the night side. Figure 4 (see also Fig. 2) illustrates such a case. It shows a near simultaneous observation of bKOM by Voyagers 1 and 2 on March 18, 1979. Voyager 1 is 13 days past Jupiter encounter at $\sim$4 hr local time while V2 is on the sunward side of Jupiter at $\sim$9 hr local time. The approximate 2 hr lapse from V1 detection of the event to V2 detection corresponds to the time required for Jupiter to rotate through the local time difference of the two spacecraft. As indicated by the black and white code, bKOM is LH polarized as seen by V2 as expected, but it is RH polarized as measured by V1. Thus, the observation of bKOM polarized in the LH sense is limited to the V1 and V2 before-encounter geometries, that is, to Jupiter local times ranging from approximately 9 hr to 10 hr. After encounter, corresponding to local times near 4 hrs, the polarization sense is reversed. The more recent post-encounter V2 polarimetric measurements, made at local times near 3 hr, support this observation.

Figures 1 and 4 display the polarization sense but they do not show d, the degree of polarization (ratio of polarized to random plus polarized power), or R, the axial ratio (ratio of wave minor to major axis). Since we measure only the left and right circular components of the wave, and not its linear components or their phase difference, individual measurements do not permit separation of d and R. With the long-term accumulation of measurements, however, d and R become separable to an extent dependent on the range of values measured. This approach allows us to set upper and lower limits on these important wave parameters and so specify the time-averaged polarization state of bKOM.

In Figure 5 we show the distribution of axial ratios measured by the Voyager 2 and 1 spacecraft before and after encounter, respectively. Each distribution is made up of approximately 1000 individual 48-sec-average measurements, and in order to minimize effects which would artificially broaden the distributions, weaker events ($\leq 10^{-21}$ W m^{-2} Hz^{-1}) were excluded. With the exception of corrections for wave incidence on the frontside or backside of the antenna, the measured values are otherwise uncorrected for antenna orientation relative to the radio source. They are thus referred to here as indicated axial ratios, R_i. The sign of R_i is correct, however, so the two distributions illustrate graphically the aforementioned post-encounter polarization sense reversal. Specifically, the before-encounter distribution, which is taken from V2 observations made between April 19 and May 31 at 97 kHz, consists almost entirely of LH polarized events. The after-encounter distribution, which is taken from V1 observations of KOM made between March 21 and May 23 at the same frequency, consists entirely of RH polarized events. The distributions at other frequencies in the bKOM range are very similar to those shown here.

In order to specify the true axial ratio of the waves, the distributions shown in Figure 5 must be transformed by functions which depend on antenna orientation, degree of polarization, and wave tilt angle -- only the first of which is known *a priori*. The distributions shown in Figure 5 are sufficiently well defined, however, that meaningful bounds may be placed on R and d, provided we interpret the results as

indicative of only the average properties of the waves. For example, examination of the curves (not shown) relating these functions indicates that for any value of true axial ratio or tilt angle, the degree of polarization must exceed about 0.75 in order to obtain the before-encounter distribution and about 0.85 to obtain the after-encounter distribution. In other words, if on the average d were less than these values, no combination of wave tilt angle or axial ratio could reproduce a distribution of R_i with mean values and standard deviations similar to those actually measured. We conclude that bKOM emission must be strongly polarized with a degree of polarization of at least 0.75.

It is also possible to similarly limit R, the true wave axial ratio; however, the bounds are less restrictive. We can only say with assurance that the waves cannot be linearly or even highly elliptically polarized ($R \lesssim 0.1$). Rather, the results are consistent with waves which are moderately elliptical to circularly polarized with a high degree of polarization. Jovian radio emission observed at much higher frequencies ($\gtrsim$ 10 MHz) [Barrow and Morrow, 1968; Kennedy, 1969] has very similar polarization characteristics.

Thus far in this section we have restricted attention to the polarization of the "north pole" bKOM, which is by far the dominant feature on the PRA dynamic spectra below about 500 kHz. Less frequently, "south pole" bKOM is observed, however, which is statistically associated with a CML range centered at about 40° [Kurth et al., 1979]. Generally the polarization sense of the south pole bKOM does not appear as consistent as that of the north pole bKOM; however, this may be due to difficulty in distinguishing between true south pole bKOM and narrow-band KOM (or nKOM) [Kaiser and Desch, 1980] which it resembles and which may have different polarization characteristics. In short, we cannot yet make an unqualified statement regarding the polarization sense of this component.

Flux Density and Power

In Figure 6, we show modal and peak flux density spectra from

Voyager 2 inbound based on an analysis of an 18-day period in June 1979. This is compared with the modal spectrum derived from post-encounter V1 data taken during a 12-day period in March. Flux density spectra of bKOM events from individual 48-sec-average measurements have been presented before [Warwick et al., 1979b]; however, because the bKOM is a highly variable energy source on short (< a few days) time scales, we define here its gross statistical behavior based on a large sample size.

The modal flux density spectrum represents the most probable flux density measured at each frequency during active periods. The pre-encounter spectral peak is at 78 kHz and the flux falls off by an order of magnitude within 60 kHz on either side of this peak. Note that, inbound, bKOM is detected so rarely in our 20 kHz channel that the most probable flux density value is at threshold. On the high frequency side, the flux density of data recorded before encounter reaches threshold at about 300 kHz. Note that in contrast to pre-encounter behavior, the post-encounter mode spectrum has a different shape and represents less integrated flux. The spectral peak has shifted to 40 kHz, the high frequency cutoff is about 250 kHz, and the integrated flux is smaller by a factor of about 2.5. As we have been able to uncover no long-term variation in bKOM energy output, we suggest that this post-encounter decline is due to geometrical factors.

To give some indication of the energy variability exhibited by bKOM we show a "peak" spectrum, which is defined here as the flux density at each frequency which is exceeded only 10% of the time. The total power in this case, obtained by integrating under the flux density curves and assuming equal beaming properties, is greater than that of the modal spectrum by about 2-1/2 times. The spectral peak has shifted down one channel to 59 kHz and now emission above threshold is apparent up to 1 MHz.

A third spectrum, which is also indicative of observed bKOM variability, is implicit in this figure. This is the spectrum represented by the detection threshold (lower, dashed) curve itself. At times bKOM disappears entirely, falling to some level below our detection

capability. On these occasions, the total power is at least several orders of magnitude below the mode, assuming once again that beaming conditions have not changed.

Using the same data set which formed Figure 6, we can compute the total power emitted by bKOM radiation by integrating over the emission bandwidth. If we assume for the sake of calculation that the radiation is emitted isotropically into space, then the measured flux density can be converted into power (isotropic), an assumption which in general yields the maximum estimate of power output. Of course it is unlikely, in view of the evidence presented in the section on occurrence statistics, that the radiation is actually emitted isotropically, but on the other hand it is also unlikely that we ever actually record the peak flux from the source if it is in fact highly beamed. At the very least, then, the results lend themselves to comparisons with the power levels of other types of emission from Jupiter and earth.

The results of computing the power in this way are as follows: the most probable isotropic power level of bKOM is about 8×10^8 watts with relatively few events surpassing this level compared with those which are less intense. Only 10% of the events measured exceeded 2×10^9 watts and less than 1% were in excess of 5×10^9 watts. (In a previous paper [Warwick et al., 1979a] based on a preliminary analysis we erroneously assigned a value of 10^{10} watts to bKOM.)

By comparison with other sources of planetary radio emission, KOM appears approximately midway in intensity between TKR (terrestrial kilometric radiation) and the high frequency component of the Jovian emission or DAM. The median power level of TKR, computed using a broad but not isotropic beam, is equal to 3×10^7 watts [Kaiser and Alexander, 1977]. Typical power levels for DAM and in particular the intense millisecond component of DAM are far in excess of 10^9 watts for even narrowly confined beams [Warwick, 1970].

Discussion

We have shown that the bKOM morphology changes substantially with viewing angle, as defined by Voyager 1 and 2 pre- and post-encounter observing geometries. Although it is not always possible to distinguish between latitude and local time effects in our results, it is clear that both the polarization sense reversal and the dynamic spectrum alteration following Jupiter encounter are effects imposed by a change in the observer's local time from essentially a dayside to a nightside perspective. These strong day-night asymmetries bear fundamentally on the nature of the bKOM source.

In regard to source models, Warwick et al. (1979b) and Green and Gurnett (1980) have suggested that KOM is generated in the magnetoionic ordinary mode at relatively low altitudes above the Jovian auroral regions. Green and Gurnett (1980) show further that the characteristic tapered dynamic spectral shape would be a natural consequence of refraction by the Io plasma torus of KOM emission generated at 2 f_p along an L = 6 field line. In both of these models it was envisioned that the KOM source either rotates with the planet or is uniformly distributed throughout all Jovian longitudes. Where we depart from this scenario is solely in regard to the latter point. Specifically, we believe that the polarization reversal and altered dynamic spectrum following encounter are consistent only with a source region which is fixed in local time. Otherwise, as the aforementioned models would predict, there should be little or no day-night asymmetry. Those models would imply that the polarization sense and dynamic spectrum should remain unaltered regardless of observing perspective, provided the latitude remained roughly constant.

With the source region fixed in local time, however, the polarization reversal could result from differences between the dayside and nightside of a bKOM beam. On the dayside the observer could be viewing the forward (main) lobe of the bKOM emission pattern, whereas the nightside observer would have to view over the pole of the planet to see the back lobe of the beam. The north pole bKOM propagation vector would have a component parallel to the magnetic field in the former case, so that ordinary mode emission appears LH polarized, as observed. In the

latter case, propagation is essentially antiparallel to the magnetic field in the northern hemisphere so that ordinary mode emission is RH polarized, again as observed. The drastic alteration in the characteristic dynamic spectrum, although not as simply explained, might reasonably be a consequence of severe refraction or planetary shadowing effects on the back lobe of the radiation pattern. Implicit in this view is the conclusion that the source is located on the planet's day side. If this model is correct, then Jupiter has an analog in the earth, as the earth's naturally occurring radio emission is known to be beamed into conical configurations centered at high latitudes and fixed in both local time and magnetic latitude (Green et al., 1977; Alexander and Kaiser, 1976). More detailed modeling of the bKOM beam pattern and source location, capable of accounting for the complex morphology described in this work, is in progress.

Acknowledgments

One of us (MDD) received support as a National Research Council post-doctoral associate.

REFERENCES

Alexander, J. K. and M. L. Kaiser, Terrestrial kilometric radiation, 1., Spatial structure studies, J. Geophys. Res., 81, 5948, 1976.

Barrow, C. H. and D. P. Morrow, The polarization of the Jupiter radiation at 18 MHz, Astrophys. J., 152, 593, 1968.

Green, J. L. and D. A. Gurnett, Ray tracing of Jovian kilometric radiation, submitted to Geophys. Res. Lett., 1979.

Green, J. L., D. A. Gurnett and S. D. Shawhan, The angular distribution of auroral kilometric radiation, J. Geophys. Res., 82, 1825, 1977.

Kaiser, M. L. and J. K. Alexander, Terrestrial kilometric radiation: 3. Average spectral properties, J. Geophys. Res., 82, 3273, 1977.

Kaiser, M. L. and M. D. Desch, Narrow-band Jovian kilometric radiation: A new radio component, submitted to Geophys. Res. Lett., 1980.

Kennedy, D. J., Polarization of the decametric radiation from Jupiter, Ph.D. thesis, University of Florida, 1969.

Kurth, W. S., D. D. Barbosa, F. L. Scarf, D. A. Gurnett, and R. L. Poynter, Low frequency radio emissions from Jupiter: Jovian kilometric radiation, Geophys. Res. Lett., 6, 747, 1979.

Kurth, W. S., D. A. Gurnett, and F. L. Scarf, Spatial and temporal studies of Jovian kilometric radiation, submitted to Geophys. Res. Lett., 1979.

Scarf, F. L., D. A. Gurnett, and W. S. Kurth, Jupiter plasma wave observations: An initial Voyager 1 overview, Science, 204, 991, 1979.

Warwick, J. W., Particles and fields near Jupiter, NASA CR-1685, 1970.

Warwick, J. W., J. B. Pearce, R. G. Peltzer, and A. C. Riddle, Planetary radio astronomy experiment for the Voyager missions, Space Sci. Rev., 21, 309, 1977.

Warwick, J. W., J. B. Pearce, A. C. Riddle, J. K. Alexander, M. D. Desch, M. L. Kaiser, J. R. Thieman, T. D. Carr, S. Gulkis, A. Boischot, C. C. Harvey and B. M. Pedersen, Voyager 1 planetary radio astronomy observations near Jupiter, Science, 204, 955, 1979a.

Warwick, J. W., J. B. Pearce, A. C. Riddle, J. K. Alexander, M. D. Desch, M. L. Kaiser, J. R. Thieman, T. D. Carr, S. Gulkis, A. Boischot, Y. Leblanc, B. M. Pedersen, and D. H. Staelin, Planetary radio astronomy observations from Voyager 2 near Jupiter, Science, 206, 991, 1979b.

FIGURE CAPTIONS

Figure 1. Voyager-2 dynamic spectrum of Jovian radio emission in the 1300 to 20 kHz frequency band. Total power is shown in the bottom panel with increasing darkness proportional to increasing intensity. The upper panel is the polarization version of the same data with white (black) representing RH (LH) polarized emission. In this 72-hr period, eight consecutive broadband (bKOM) events are visible, each LH polarized and coincident with the tic marks indicating magnetic north dipole tip passage ($\sim 200^{\circ}$ CML). Characteristic of pre-encounter signatures (cf. Fig. 2), the bKOM events are roughly tapered in appearance, lasting longer at lower frequencies. The events are anticoincident with the hectometer-wavelength (HOM) emission, which is strongest at higher frequencies.

Figure 2. Voyager 1 dynamic spectrum of a 24-hr period on April 8, 1979, in the same format as that of Figure 1. V1 is now 34 days past encounter with Jupiter. Three bKOM events are visible, each only approximately coincident with north dipole tip passage ($\sim 200^{\circ}$ CML). Unlike typical pre-encounter spectra, however, only one of the events, the first at 0 to 04 hr SCET, is tapered in appearance. The other two, at approximately 12 hr and 22 hr SCET, typify the spectral appearance of post-encounter data. These events reach a maximum both in frequency and intensity near 150° CML (instead of 200°), and exhibit a secondary emission region near 240° CML. Near 200° CML, approxixmately coincident with the tic marks, little or no emission is recorded. Note that the events are RH polarized. A type III burst is also visible in this figure, beginning at 1315 hr and drifting from 1.3 MHz down to 2 00 kHz.

Figure 3. Time line (bottom panels) and histogram (top panels) representations of the bKOM occurrence statistics. The unshaded (shaded) histograms include only those events exceeding a normalized flux density of 2.5×10^{-22} (2.5×10^{-21}) W m^{-2} Hz^{-1}. The data are organized according to observing perspective, with the V1 pre-encounter data covering the period from Dec. 15, 1978 through

Feb. 28, 1979; V2 pre-encounter from Apr. 10, 1979 through May 31, 1979; V1 post-encounter from Mar. 10, 1979 through May 28, 1979. The detection of bKOM is always highest in the longitude sector centered on about 200° CML regardless of observing geometry; however, the occurrence signature of post-encounter data differs markedly from pre-encounter activity. The time-line plots show no significant accumulation of activity at any Io phase locations.

Figure 4. Polarization plot showing detection by both Voyagers of the same, but oppositely polarized, bKOM event on March 18, 1979. Polarization convention is the same as that of Figure 1 so that the event is RH polarized as seen by V1 (top panel, 08 to 12 hr SCET) and LH polarized as seen by V2 (bottom panel, 10 to 14 hr SCET). The V1 observation is from a vantage point near 4 hr local time on the night side of the planet while V2 is near 9.5 hr local time on the day side.

Figure 5. Statistical distribution of 48-sec-average bKOM events according to their indicated axial ratio. The before-encounter distribution is taken from V2 observations made from Apr. 19, 1979 through May 31, 1979. The after-encounter observations were made by V1 from Mar. 21, 1979 through May 23, 1979. The shift from predominantly LH to RH polarized emission after encounter is clear. Radiation incidence on the frontside or backside of the antenna has been accounted for in defining the sign of the axial ratio.

Figure 6. Statistical (normalized) flux density spectra of bKOM emission. The top two (solid) curves are from V2 observations made from June 5, 1979 through June 22, 1979. The "peak" spectrum represents the flux density exceeded only 10% of the time at a given frequency. The modal spectrum represents the most probable or commonly occurring flux density measured at a given frequency. The integrated flux or power represented by these two curves, assuming isotropic beaming of radiation into 4π steradian of solid angle, is equal to 2×10^{9} and 8×10^{8} watts, respectively. The post-encounter mode spectrum (dashed curve), taken from V1 observations made from

Mar. 10, 1979 through Mar. 21, 1979, shows the shift in the frequency of peak flux from 78 to 40 kHz and a decline in the total integrated flux relative to pre-encounter. Flux densities are normalized to the standard earth-Jupiter opposition distance of 4.04 AU.

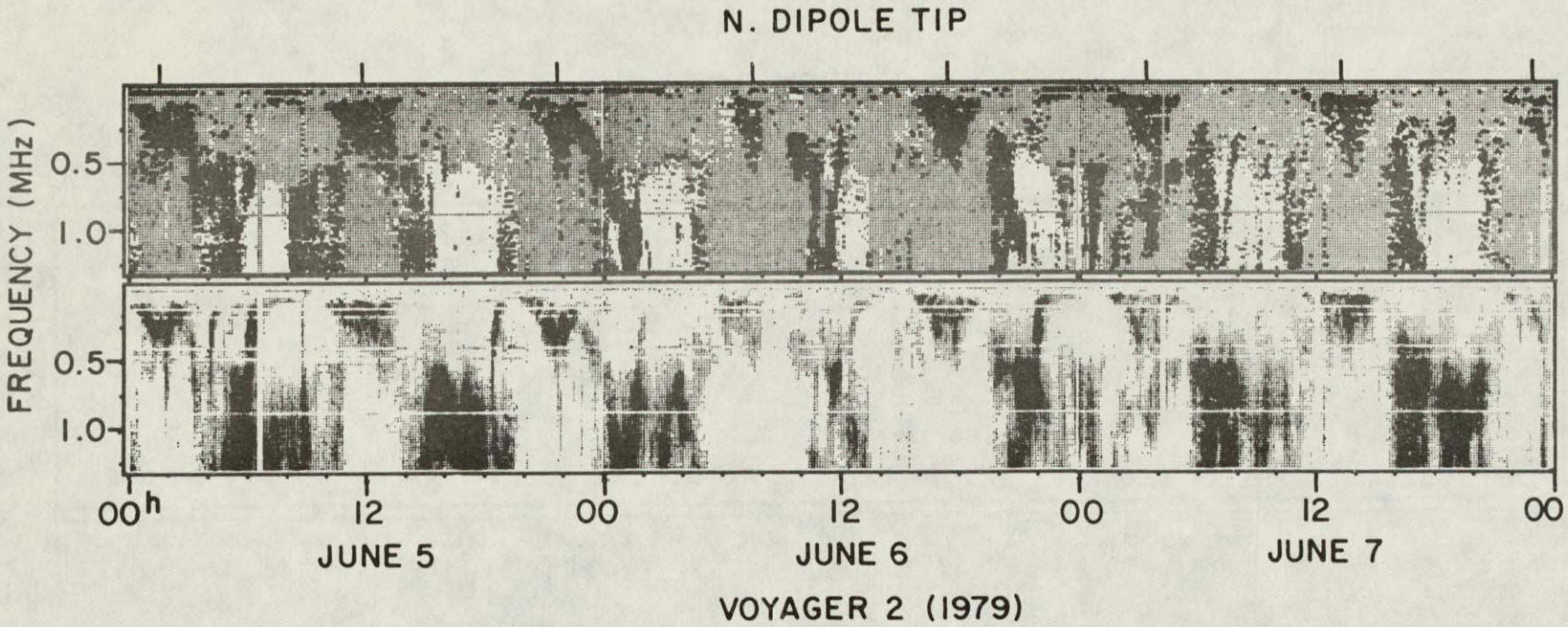
N. DIPOLE TIP
FREQUENCY (MHz)
0.5
1.0
0.5
1.0
00h
12
00
12
00
12
00
JUNE 5
JUNE 6
JUNE 7
VOYAGER 2 (1979)

Figure 1

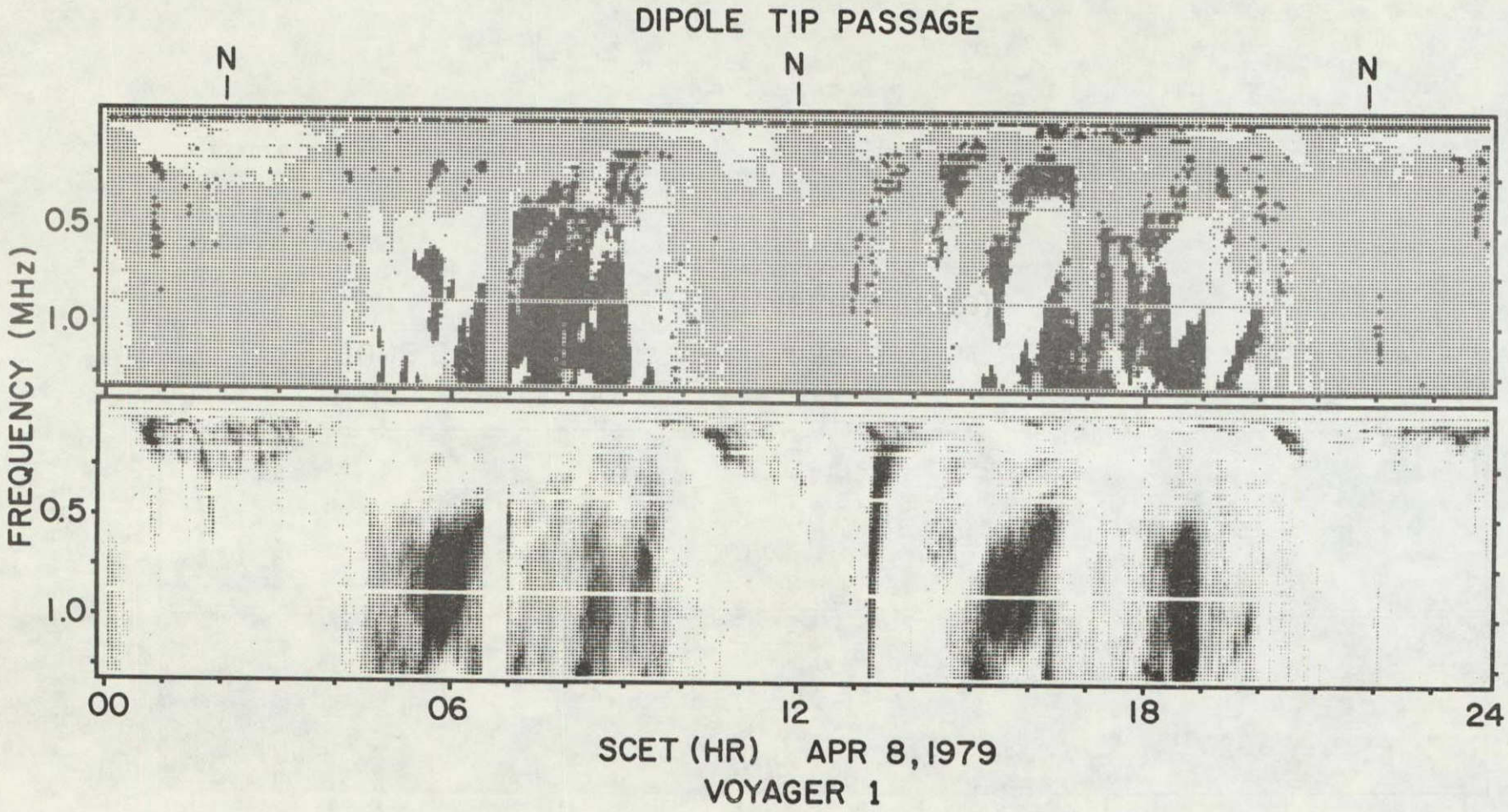
DIPOLE TIP PASSAGE
N
N
N
FREQUENCY (MHz)
0.5
1.0
0.5
1.0
00
06
12
18
24
SCET (HR) APR 8, 1979
VOYAGER 1

Figure 2

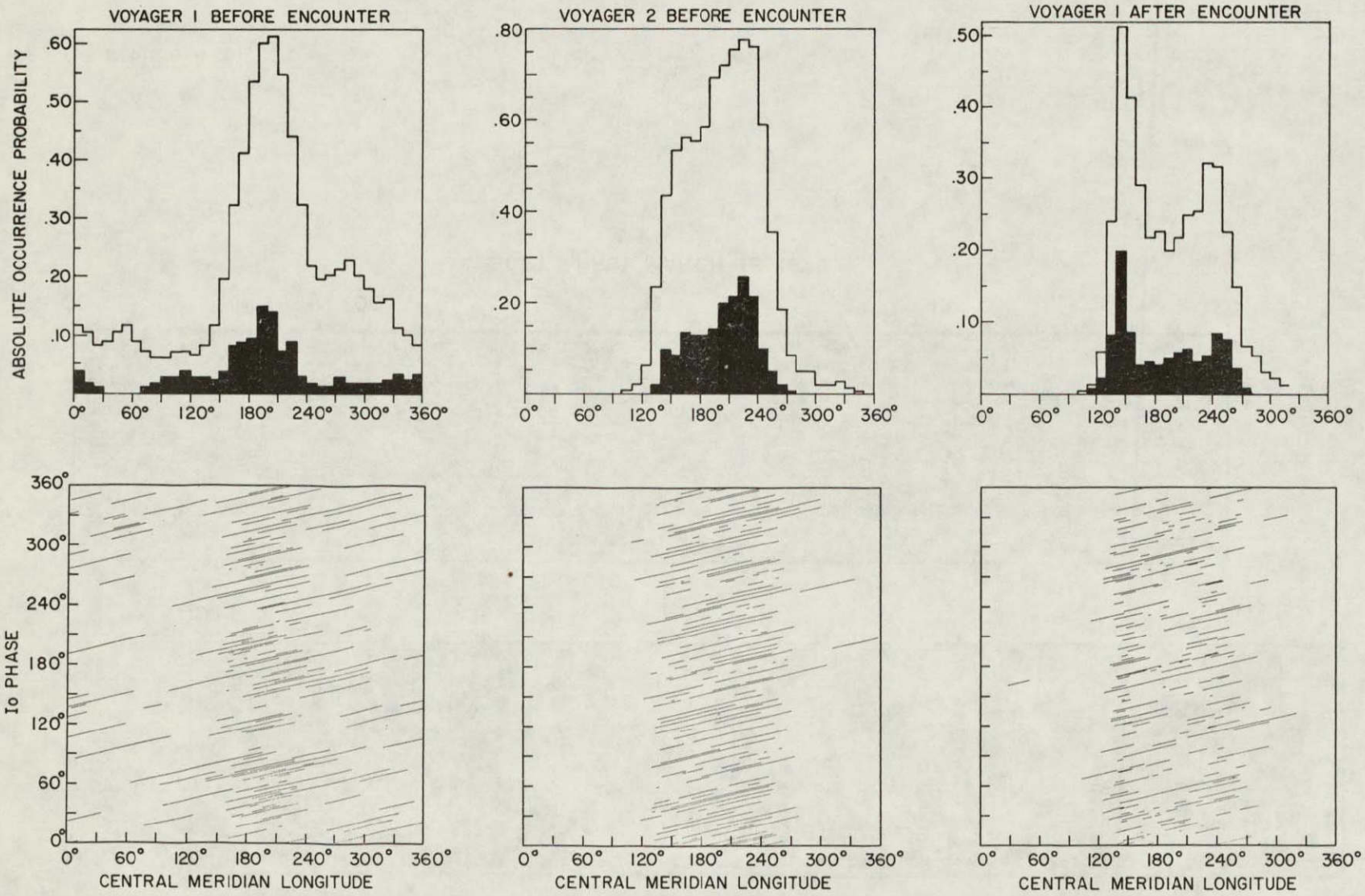
VOYAGER 1 BEFORE ENCOUNTER
VOYAGER 2 BEFORE ENCOUNTER
VOYAGER 1 AFTER ENCOUNTER
ABSOLUTE OCCURRENCE PROBABILITY
.60
.50
.40
.30
.20
.10
.80
.60
.40
.20
.50
.40
.30
.20
.10
0° 60° 120° 180° 240° 300° 360°
Io PHASE
360°
300°
240°
180°
120°
60°
0°
CENTRAL MERIDIAN LONGITUDE

Figure 3

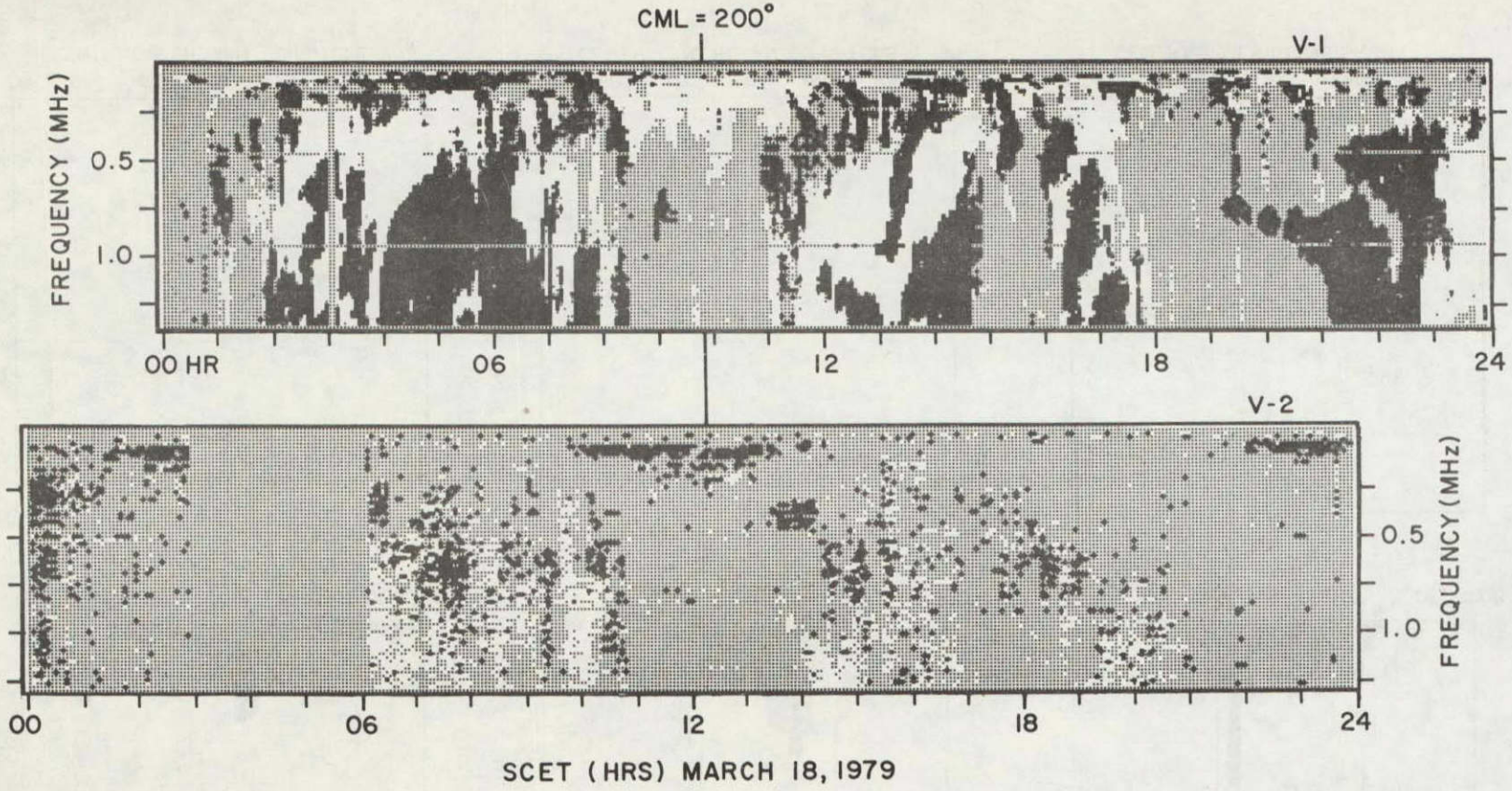
CML = 200°
V-1
FREQUENCY (MHz)
0.5
1.0
00 HR
06
12
18
24
V-2
FREQUENCY (MHz)
0.5
1.0
00
06
12
18
24
SCET (HRS) MARCH 18, 1979

Figure 4

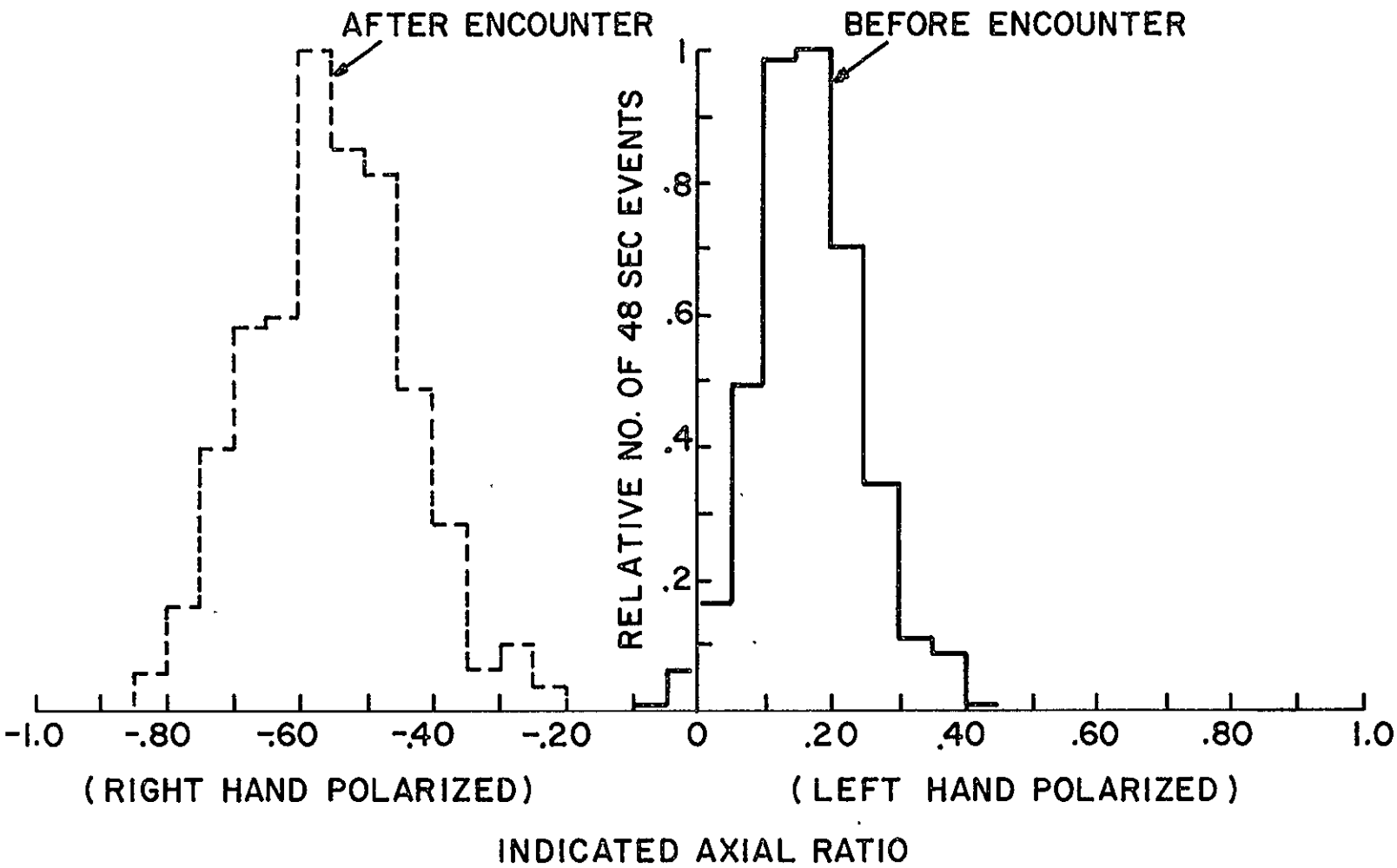
AFTER ENCOUNTER
BEFORE ENCOUNTER
RELATIVE NO. OF 48 SEC EVENTS
1
.8
.6
.4
.2
-1.0
-.80
-.60
-.40
-.20
0
.20
.40
.60
.80
1.0
(RIGHT HAND POLARIZED)
(LEFT HAND POLARIZED)
INDICATED AXIAL RATIO

Figure 5

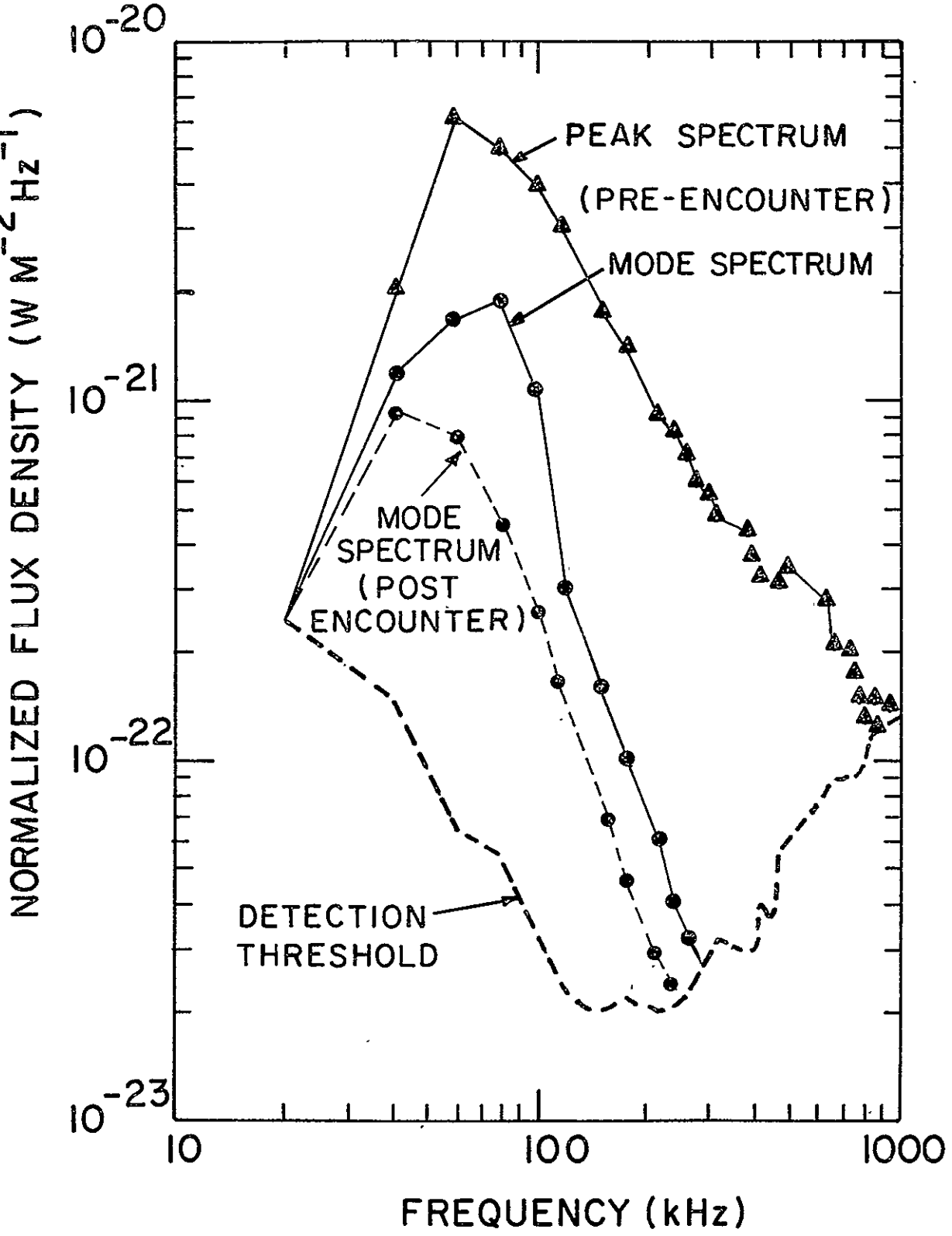
10^{-20}
10^{-21}
10^{-22}
10^{-23}
NORMALIZED FLUX DENSITY ($W\,M^{-2}\,Hz^{-1}$)
PEAK SPECTRUM
(PRE-ENCOUNTER)
MODE SPECTRUM
MODE
SPECTRUM
(POST
ENCOUNTER)
DETECTION
THRESHOLD
10
100
1000
FREQUENCY (kHz)

Figure 6

BIBLIOGRAPHIC DATA SHEET

1. Report No.	2. Government Accession No.	3. Recipient's Catalog No.
TM 80627		

4. Title and Subtitle	5. Report Date
The Occurrence Rate, Polarization Character and Intensity of Broadband Jovian Kilometric Radiation	January 1980
	6. Performing Organization Code: 695
7. Author(s): M. D. Desch and M. L. Kaiser	8. Performing Organization Report No.
9. Performing Organization Name and Address: Goddard Space Flight Center, Greenbelt, Maryland 20771	10. Work Unit No.
	11. Contract or Grant No.
	13. Type of Report and Period Covered: Technical Memorandum
12. Sponsoring Agency Name and Address	14. Sponsoring Agency Code

15. Supplementary Notes

16. Abstract

We describe the major observational features of one new component of Jupiter's radio emission spectrum, the broadband kilometer-wavelength radiation or bKOM. This study, using the Voyager Planetary Radio Astronomy experiment, reveals that the overall occurrence morphology, total power, and polarization character of bKOM are strong functions of the latitude and/or local time geometry of the observations. The post-encounter data show a decline in the mean occurrence rates and power level of bKOM and, in particular, a depletion in the occurrence rate at those same longitudes where the detection rate is a maximum before encounter. Additionally, the polarization sense undergoes a permanent reversal in sign after encounter, whereas the time-averaged wave axial ratio and degree of polarization remain relatively unchanged. Finally, no evidence of any control by Io is found. The strong dependence of the morphology on local time suggests a source whose beam is nearly fixed relative to the Jupiter-sun line.

17. Key Words (Selected by Author(s))	18. Distribution Statement
Jupiter, radio emission, Voyager spacecraft	

19. Security Classif. (of this report)	20. Security Classif. (of this page)	21. No. of Pages	22. Price*
U	U	23	

*For sale by the National Technical Information Service, Springfield, Virginia 22151.